Manipulating cellular interactions of poly(glycidyl methacrylate) nanoparticles using mixed polymer brushes.

Tristan D. Clemons,[a*] Michael Challenor,[a,b] Melinda Fitzgerald,[b] Sarah A. Dunlop,[b] Nicole M. Smith[a,b] and K. Swaminathan Iyer[a*]

a. School of Chemistry and Biochemistry, University of Western Australia, 35 Stirling Hwy, Crawley, WA 6009, Australia. E-mail: TDC: tristan.clemons@uwa.edu.au or KSI: swaminatha.iyer@uwa.edu.au.

b. Experimental and Regenerative Neurosciences, School of Animal Biology, University of Western Australia, 35 Stirling Hwy, Crawley, WA 6009, Australia.

ABSTRACT: There is a growing need for the development of nanoparticles, with imaging and drug delivery capabilities, to maintain cellular uptake but avoid protein attachment and recognition. In this study we have demonstrated that nanoparticles consisting of a poly(glycidyl methacrylate) (PGMA) core and a mixed brush architecture of methoxypoly(ethylene glycol) and poly(ethylenimine) (mPEG-PEI) on the surface can meet this need. Surface functionalization with PEI alone results in cellular uptake but rapid protein attachment and PEG alone can avoid protein attachment but to the detriment of cellular uptake. A mixed copolymer brush of both PEI and mPEG provides the ideal balance.

The application of nanoparticles for imaging and drug delivery is highly dependent on the ability to tailor the nanoparticles interactions with cells.[1] These interactions are pivotal in determining intracellular retention of the drugs and imaging agents within the target tissue. It is widely accepted that, compared to anionic or neutral nanoparticles, a cationic surface charge results in enhanced cell penetration owing to favorable interactions with the negatively charged cellular plasma membrane.[2] Furthermore, following intravenous administration, cationic nanoparticles are rapidly sequestered by the mononuclear phagocyte system (MPS) consisting of dendritic cells, blood monocytes, and tissue-resident macrophages in the liver, spleen, and lymph nodes, which are responsible for clearing these materials from circulation.[3] Clearance is in turn dependent on the adsorption of plasma proteins on the cationic nanoparticle surface.[4] This adsorption of proteins on the nanoparticle surface, often referred to as a protein corona, can significantly alter the biological identity of the nanoparticle and in turn can have dramatic effects on potential biomedical applications and toxicology.[5] The formation of the protein corona can be defined in the early phase as a 'soft' corona with serum proteins loosely bound to the nanoparticle surface and in equilibrium with free surrounding serum proteins.[6] This soft corona can be easily displaced or stripped from the nanoparticle surface if the surrounding serum protein concentration was to decrease. This is in contrast to a 'hard' protein corona where proteins lower in abundance but high in affinity for binding to the nanoparticle surface will begin to adsorb over time developing a persistent and more permanent protein coating.[6] This study will mainly focus on the acute interactions with proteins of 3 polymeric nanoparticles with modified surfaces and the effects this has on the nanoparticle cellular uptake. Proteins that bind to a nanoparticle surface act as opsonins that mark a nanoparticle for efficient uptake by the MPS and subsequent nanoparticle clearance.[3b, 7] Previous studies have shown that adsorption of proteins onto the nanoparticle surface reduces the nanoparticle's ability to adhere to the cell membrane, resulting in reduced cellular uptake.[8] PEGylation of nanoparticle surfaces is commonly used to block protein adsorption.[9] The ability of PEG coatings to prevent protein adsorption is attributed to steric repulsion, resulting from loss of conformational freedom of PEG chains as they become compressed when the protein approaches the surface.[10] However, enhancement of circulation times using PEGylation also prevents active interaction and endocytosis in target cells.[11] In the present study using a "grafting to" approach to a colloidal poly(glycidyl methacrylate) (PGMA) nanoparticle core, we systematically demonstrate that whilst reducing protein adsorption on the nanoparticle surface it is possible to maintain active endocytosis of the nanoparticles using a mixed brush strategy incorporating both PEI and mPEG (Figure 1, and Supporting information Figure S1).

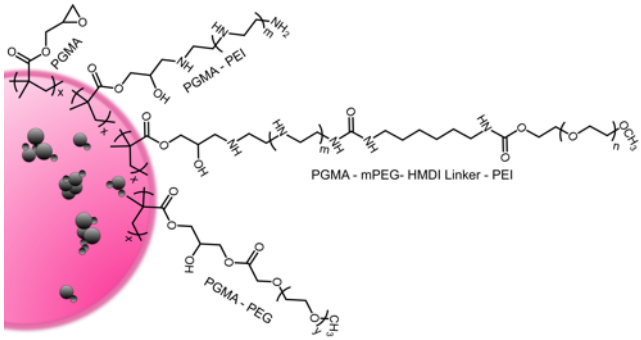

Figure 1. Schematic representation of the PGMA polymer nanoparticles and the surface modifications investigated for this study, PEI, mPEG-PEI and PEG.

The nanoparticles used in the current study consist of a rhodamine B-PGMA core (RhB-PGMA, see supporting information, Figure S1 for reaction scheme) containing encapsulated magnetite (Fe_3O_4) nanoparticles (Figure 2A) prepared from an oil in water emulsion process. The iron content of the nanoparticles was determined to be 2.5% w/w by ICP-AES. RhB functionalization of the nanoparticles enabled tracking of the nanoparticle cellular interactions with fluorescence microscopy. The presence of Fe_3O_4 provides a means to separate, wash excess surfactant and reactants, as well as concentrate the nanoparticles using a magnetic fractionation column following surface modification of the PGMA core. Furthermore, Fe_3O_4 encapsulation also provides the potential for MRI contrast *in vivo* and cellular maneuverability of internalized nanoparticles with a magnetic field, which have been demonstrated in previous studies recently.[12] Both the fluorescent and magnetic capabilities of the nanoparticle cores have been demonstrated in culture, *ex vivo* and in *in vivo* studies previously.[12-13] Importantly, the glycidyl methacrylate units, located in the "loops" of the PGMA core and containing multiple free epoxy groups, serve as reactive sites for subsequent grafting of polymer chains. It has been demonstrated that increased mobility of the polymer chains in the PGMA core ensures better access to the epoxide functional groups, resulting in a 2- to 3-fold greater grafting density when compared with a monolayer of epoxy groups on a nanoparticle surface of similar dimension.[14] In the current study we analyzed grafting of short chain branched PEI, linear PEG and mPEG-PEI (linear PEG with a branched PEI) copolymer to the PGMA-RhB core (See supporting information Figure S2-S4). PEI was chosen as a cationic polymer as it is the most widely used non-viral polymeric transfection agent.[15] However, despite efficient transfection, these particles are also subject to rapid protein identification and in turn potential premature clearance *via* the MPS system.[3b]

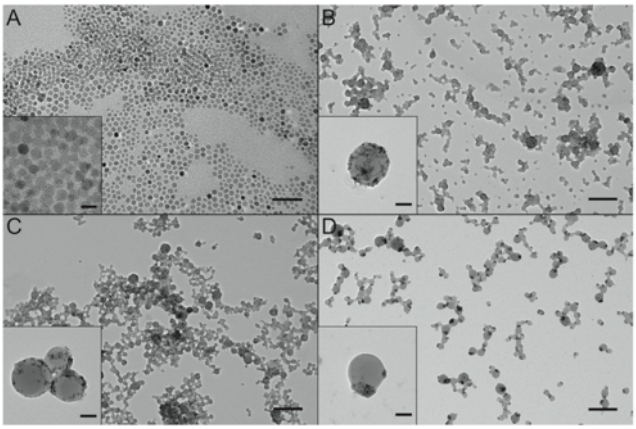

Figure 2. Transmission electron microscopy of (A) magnetite nanoparticles with high magnification inset (scale 50nm and inset 10nm), (B) PEI decorated PGMA nanoparticles with high magnification inset, (C) PEG-decorated PGMA nanoparticles with high magnification inset and (D) mPEG-PEI-decorated PGMA nanoparticles with high magnification inset. Scales for B-D are 500nm with inset scale 50nm.

The 3 nanoparticle systems used in this study were analyzed by dynamic light scattering (DLS) and found to have comparable hydrodynamic radii of approximately 150 nm (See supporting information, Figure S5 and Table S1), a finding supported by transmission electron microscopy (Figure 2). Despite identical solvent conditions during the emulsion process of each nanoparticle the distribution of the Fe_3O_4 is very different in all 3 systems. This suggests that polymer differences and the variability in the stability of the emulsion generated during sonication plays an important role in the Fe_3O_4 encapsulation. When analyzed in milli-Q water, the zeta potential of the nanoparticles was highest for PEI-decorated nanoparticles (52.9 mV), followed by mPEG-PEI-decorated (29.0 mV) and finally the PEG-decorated (-29.9 mV) nanoparticles (See supporting information, Figure S4 and Table S1). Nanoparticle samples were also assessed by DLS in the presence of both bovine serum albumin (BSA) and 10% human serum. In the presence of both BSA and human serum, all nanoparticle systems experienced an increase in hydrodynamic radii due to interactions with the serum proteins. Furthermore, all nanoparticles experienced a decrease in the absolute magnitude of the observed zeta potential (see supporting information, Table S1) in the presence of the serum proteins. This data taken together suggests a favourable interaction between the serum proteins and all nanoparticle systems investigated in this study.

Cellular toxicity of these nanoparticle platforms was assessed *in vitro* using rat pheochromocytoma neural progenitor (PC12) cells. All 3 nanoparticle systems displayed no cellular toxicity *in vitro* up to a maximum concentration of 250 $\mu g\ mL^{-1}$ (See supporting information Figure S6). PEI alone has been shown to be cytotoxic, with the cellular toxicity increasing as the molecular weight of the PEI increases.[16] We have found that the short chain PEI used in this study for the PEI decorated nanoparticles and others, combined with anchoring the PEI to the nanoparticle core, is able to alleviate the associated toxicity often seen with free PEI polymer chains.[17] Furthermore, previous studies have shown 25 kDa PEI to induce membrane damage and initiate apoptosis *in vitro*[16b] however this was not evident in our work with the mPEG-PEI decorated nanoparticles. This again suggests that the anchoring to a nanoparticle substrate as well as the mPEG polymer coverage plays a protective role with respect to cell toxicity. Confocal microscopy of PC12 cells following 24h incubation with the nanoparticles was used to investigate the cellular uptake of each nanoparticle platform. Following washing to remove excess nanoparticles, images were collected from a single visual slice on the confocal through the midsection of the cells to ensure nanoparticles present were truly intracellular. The PEI-decorated nanoparticles were readily internalized by cells, as expected and consistent with previous reports from our group (Figure 3A).[12b, 13, 17] Similarly the PEG-decorated PGMA nanoparticle also behaved as expected, with no significant cellular association or uptake following the 24h incubation period (Figure 3B). The mPEG-PEI-decorated nanoparticles showed similar results to that of the PEI nanoparticles, with strong cellular association and uptake regardless of the presence of serum in the incubation media (Figure 3C and 3D). Hence, despite the presence of serum proteins and the incorporation of the mPEG polymer on the nanoparticle surface, favorable cellular interactions can still be achieved with this mixed brush strategy.[2d]

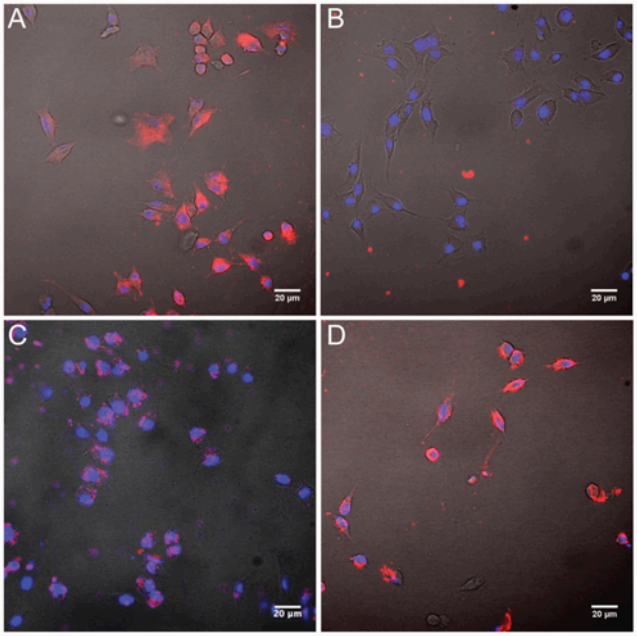

Figure 3. Confocal assessment of cellular uptake of nanoparticle preparations by PC12 cells following 24h incubation: A) PEI coated nanoparticles, B) PEG coated nanoparticles, C) mPEG-PEI coated nanoparticles, all in growth medium, and D) mPEG-PEI decorated nanoparticles in the absence of serum in the media. All nanoparticle suspensions were at a final concentration of 20 µg-mL-1, all scale bars are 20 µm. All images are bright field images with fluorescence from Rhodamine B labeled nanoparticles (red) and Hoechst stained nuclei (blue).

Further to the assessment of cellular uptake in the neuronal culture conditions, cellular uptake in a phagocytic cell line was assessed in order to evaluate the effect of differing nanoparticle surfaces on phagocytosis. Nanoparticle uptake in ramified (non-activated) microglia was compared to uptake by lipopolysaccharide (LPS) activated microglia (assessed *via* ED-1 immunoreactivity, see supporting information Figure S7). The addition of LPS to cell cultures has long been established as a method for activating microglia into a phagocytic inflammatory state.[18] Similar to the neuronal assessment, PEI-decorated nanoparticles were internalized by both activated and non activated microglia (Figure 4A and B), PEG-decorated nanoparticles experienced effectively no cellular uptake by both activated and non activated microglia (Figure 4C and D) and the mPEG-PEI-decorated nanoparticle uptake was again evident in both the activated and non activated microglia (Figure 4E and F).

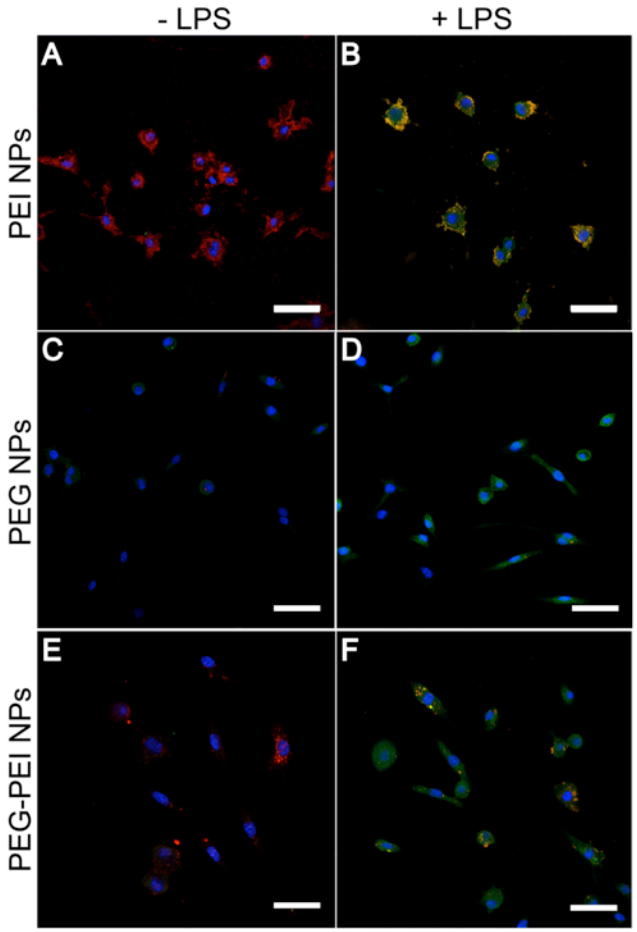

Figure 4. Confocal assessment of cellular uptake of nanoparticle preparations by LPS activated and non activated microglia following 24h incubation: A) PEI-decorated nanoparticles, B) PEI-decorated nanoparticles with LPS stimulation, C) PEG-decorated nanoparticles, D) PEG-decorated nanoparticles with LPS stimulation, E) mPEG-PEI-decorated nanoparticles, F) mPEG-PEI-decorated nanoparticles with LPS stimulation. Nanoparticles labeled with Rhodamine B (red), ED-1 to assess microglial activation (green), Hoechst (blue), all scale bars are 50 µm.

Finally, to assess the nanoparticle's ability to avoid protein adsorption and mimic opsonin identification in the body, nanoparticles were incubated with bovine serum albumin (BSA) to assess the degree of protein binding. BSA is an ideal model protein for this experiment, as it is a common and abundant globular serum protein with many similar characteristics to that of human serum albumin and its potential binding with nanoparticles.[19] It was found that the highly cationic PEI coated nanoparticles significantly bound a large proportion of the BSA present (Figure 5), leading to nanoparticle instability and aggregation within 30 minutes. As expected, the PEGylated nanoparticles were able to avoid protein binding across all time points out to 5h. The mPEG-PEI copolymer decorated nanoparticles were also able to avoid aggregation and significant BSA adsorption across the 5h time frame. For the mPEG-PEI decorated nanoparticles the percentage of bound BSA on the nanoparticles was 5.4%, 1.5% and 3.6% at 0.5h, 2h and 5h respectively. Taken together, our data suggest that a mPEG-PEI nanoparticle platform is able to achieve cellular uptake while also avoiding ubiquitous protein adsorption. Together these results provide promise for a nanoparticle platform suit-

able for intracellular delivery of therapeutics while being able to avoid premature protein recognition and clearance.

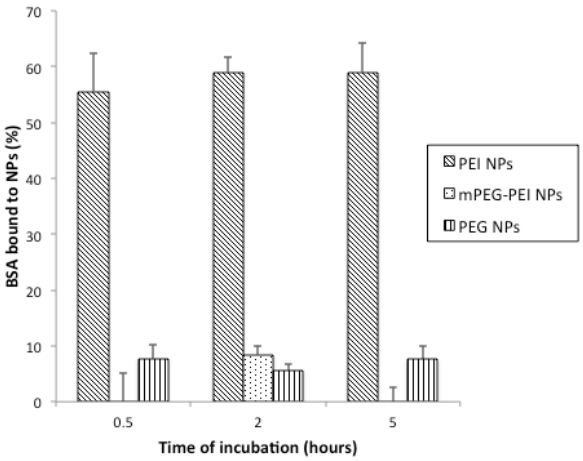

Figure 5. Time course assessment of bovine serum albumin (BSA) binding to the PEI, PEG or mPEG-PEI decorated nanoparticles. Data displayed as mean ± standard error of n=3 measurements.

In summary, we have demonstrated that through systematic modification of a PGMA core with a mixed polymer brush surface architecture, we can achieve both cellular uptake of the nanoparticle while minimizing protein interaction on the nanoparticle surface. This is an important finding for the development and use of similar polymeric nanoparticles for biological applications.

EXPERIMENTAL

Nanoparticle synthesis and characterization

All nanoparticles were synthesized making use of an emulsion synthesis protocol described previously and detailed in full in the electronic supplementary information.[17] FTIR analysis of the mPEG-PEI copolymer was performed on a Perkin Elmer Spectrum One FT-IR Spectrometer. FTIR analysis clearly shows the expected absence of C-O ether stretching in the PEI, and the absence of amine and cyano stretches in the mPEG sample, but clearly shows the combination of these signals in the copolymer with the evolution of the C=O stretch (1660 cm^{-1}) formed during the linking process (See supporting information, Figure S1). ^{1}H NMR (500 MHz) and ^{13}C NMR (125 MHz) spectra of the copolymer were recorded on a Bruker AV500 instrument in 5 mm NMR tubes. Samples were recorded in D_2O solution in ppm and referenced to the internal D_2O singlet at 4.79 ppm. ^{13}C and ^{1}H NMR analysis of the copolymer revealed successful linking of mPEG and PEI with a hexamethylene diisocyanate (HMDI) linker (See supporting information, Figure S2). Dynamic light scattering (DLS) measurements of size and zeta potential of nanoparticle preparations were performed on a Malvern Zetasizer instrument on nanoparticle samples suspended in milli-Q water, in the presence of 0.5 mg mL^{-1} BSA or in the presence of 10% human serum. Samples prepared for transmission electron microscopy analysis were prepared by depositing onto carbon-coated grids and imaged at 120kV on a JEOL JEM-2100. The iron content of the PGMA nanoparticles was determined by ICP-AES after acid digestion (5ml).

Cell culture

PC12 neuronal cells were maintained in RPMI1640 medium containing horse serum (10%), foetal bovine serum (5%), penicillin/streptomycin (100 U mL^{-1}, 100 µg mL^{-1}), L-glutamine (2 mM), non-essential amino acids (100 µM), sodium pyruvate (1 mM) (referred to as growth medium) and were incubated in a humidified atmosphere containing 5% CO_2 at 37 °C. For experiments, cells were either seeded on 10mm coverslips for confocal assessment or 96-well plates for cellular viability assessments. All culture surfaces were coated with 0.1 mg mL^{-1} poly(L-lysine) (Sigma) and cells were plated at a cell density of 0.5 – 1 × 10^5 cells-mL^{-1}. Cells were not differentiated with NGF. EOC2 CRL-2467 microglial cells were maintained in Dulbecco's modified Eagle's medium with 4 mM L^{-1} glutamine adjusted to contain 1.5 g L^{-1} sodium bicarbonate and 4.5 g L^{-1} glucose, 70%; fetal bovine serum, 10%; LADMAC Conditioned Media (produced from the LADMAC cell line (CRL-2420), 20%. Cells were incubated in a humidified atmosphere containing 5% CO_2 at 37 °C.

Cell Viability PC12 neuronal cells

Viability was measured using a Live/Dead cell kit (Invitrogen). PC12 cells were seeded at 1 × 10^5 cells-mL^{-1} in growth media and pre incubated for 24h before the media was replaced with nanoparticle suspensions of different concentrations in growth media (n=3 minimum). Cells were incubated with nanoparticles for 24h, then washed with PBS and incubated for 30 min with 100 µL of the detection reagents (Calcein AM, 1 µM; ethidium homodimer-1, 2–3 µM). Images were recorded using an inverted fluorescence microscope at 20× magnification (Olympus IX-71, Olympus IX-81). Four images were recorded from each well at consistent locations for all wells and all experiments, and live and dead cells were counted.

Confocal analysis

PC12 neuronal cells were grown on coverslips as described above, and incubated with nanoparticles in growth media at 20 µg mL^{-1} for 24h before being washed with PBS and fixed in 4% paraformaldehyde (Sigma). Cell nuclei were visualized using Hoechst 33342 (Sigma, 1 µg-mL^{-1}) following standard protocols. Images were captured by confocal microscopy (Leica TCS SP2, Nikon A1Si). RhB was detected with a laser excitation of 516nm and an emission collection window of 570 – 620nm. Hoechst was detected with the Spectra-physics Mai-Tai multi-photon laser, pulsed and centered at 800nm with a detection collection window of 400 – 450nm. EOC2 CRL-2467 microglial cells were plated on Lab-Tek® 8-well chamber slides at a concentration of 1250 cells/well. Cells were left overnight to adhere before growth media was replaced with either fresh growth media (non stimulating) or with growth media supplemented with 100 ng ml^{-1} LPS (stimulating media) before a further 24h incubation. Control and nanoparticle solutions (control (no nanoparticles), PEI-decorated, PEG-decorated and mPEG-PEI-decorated nanoparticles), were prepared in either control growth media or in the LPS stimulating media at a final nanoparticle concentration of 20 µg ml^{-1}. Following the LPS stimulation (24h) media was removed from all wells and nanoparticle solutions in growth

media added to non-stimulated cells and nanoparticles in stimulating media added to stimulated cells. Following 24h of nanoparticle incubation, media was removed, cells washed with PBS and fixed in 4% paraformaldehyde (Sigma). Immunohistochemistry for ED1 expression, 1:500 dilution anti-CD68 [ED1] (Abcam, ab31630) primary, visualized with Alexa Fluor 488 secondary (ThermoFisher a21202) and cell nuclei were visualized using Hoechst 33342 (Sigma, 1 μg mL^{-1}), following standard protocols. Images were captured by confocal microscopy on a Nikon Ti-E inverted motorized microscope with a Nikon A1Si spectral detector confocal system running NIS-C Elements software. All samples were conducted in duplicate and n=5 images as minimum collected per treatment.

Protein attachment experiment

Triplicate samples were prepared containing 100 μg of nanoparticles (PEI, PEG, mPEG-PEI decorated nanoparticles) with 50 μg BSA in a total volume of 100 μL milli-Q H2O. Control preparations did not contain nanoparticles. Samples were incubated for either 0.5, 2 or 5h before centrifugation (14,000 rpm, 30 min) to remove nanoparticles and bound BSA. Aliquots of the supernatant were collected and measured for absorbance on a Nanodrop UV-Vis instrument where the absorbance was compared to a prepared BSA standard curve (See supporting information, Figure S8 for the standard curve). Concentration of the BSA in supernatants was calculated and percentage of BSA bound to nanoparticles determined.

ASSOCIATED CONTENT

Supporting Information

Supporting information is available which contains complete synthesis protocols for the nanoparticles used in this study as well as supporting experiments including FTIR and NMR characterization of the PEG-PEI copolymer and cellular toxicity studies with the nanoparticles. The Supporting Information is available free of charge on the ACS Publications website at DOI: 10.1021/acsmacrolett.XXXXXXX.

AUTHOR INFORMATION

Corresponding Author

*School of Chemistry and Biochemistry, University of Western Australia, 35 Stirling Hwy, Crawley, WA 6009, Australia. E-mail: TDC: tristan.clemons@uwa.edu.au or KSI: swaminatha.iyer@uwa.edu.au.

ACKNOWLEDGMENTS

The authors would like to acknowledge Ms Naina Akella, for her work on this project as a part of the WA state government run BioGENEius challenge. The authors also acknowledge the Australian Microscopy & Microanalysis Research Facility at the Centre for Microscopy, Characterization & Analysis, The University of Western Australia, funded by the University, State and Commonwealth Governments. This work was funded by the Australian Research Council (ARC), the National Health & Medical Research Council (NHMRC) of Australia and the Raine Medical Research Foundation. Tristan Clemons is a NHMRC Peter Doherty – Australian Biomedical Fellow, Melinda Fitzgerald is a NHMRC Career Development Fellow and K. Swaminathan Iyer is an ARC Future fellow.

REFERENCES

1. Mailander, V.; Landfester, K., Interaction of Nanoparticles with Cells. Biomacromolecules 2009, 10 (9), 2379-2400.
2. (a) Frohlich, E., The role of surface charge in cellular uptake and cytotoxicity of medical nanoparticles. Int. J. Nanomedicine 2012, 7, 5577-5591; (b) Nafee, N.; Schneider, M.; Schaefer, U. F.; Lehr, C. M., Relevance of the colloidal stability of chitosan/PLGA nanoparticles on their cytotoxicity profile. Int. J. Pharm. 2009, 381 (2), 130-139; (c) Shenoy, D. B.; Amiji, M. A., Poly(ethylene oxide)-modified poly(epsilon-caprolactone) nanoparticles for targeted delivery of tamoxifen in breast cancer. Int. J. Pharm. 2005, 293 (1-2), 261-270; (d) Verma, A.; Stellacci, F., Effect of Surface Properties on Nanoparticle-Cell Interactions. Small 2010, 6 (1), 12-21.
3. (a) Kumari, A.; Yadav, S. K.; Yadav, S. C., Biodegradable polymeric nanoparticles based drug delivery systems. Colloid Surface B 2010, 75 (1), 1-18; (b) Song, G.; Petschauer, J. S.; Madden, A. J.; Zamboni, W. C., Nanoparticles and the mononuclear phagocyte system: pharmacokinetics and applications for inflammatory diseases. Curr Rheumatol Rev 2014, 10 (1), 22-34.
4. (a) Liu, F.; Liu, D. X., Serum independent liposome uptake by mouse liver. Bba-Biomembranes 1996, 1278 (1), 5-11; (b) Patil, S.; Sandberg, A.; Heckert, E.; Self, W.; Seal, S., Protein adsorption and cellular uptake of cerium oxide nanoparticles as a function of zeta potential. Biomaterials 2007, 28 (31), 4600-4607.
5. (a) Casals, E.; Pfaller, T.; Duschl, A.; Oostingh, G. J.; Puntes, V., Time Evolution of the Nanoparticle Protein Corona. ACS Nano 2010, 4 (7), 3623-3632; (b) Tenzer, S.; Docter, D.; Kuharev, J.; Musyanovych, A.; Fetz, V.; Hecht, R.; Schlenk, F.; Fischer, D.; Kiouptsi, K.; Reinhardt, C.; Landfester, K.; Schild, H.; Maskos, M.; Knauer, S. K.; Stauber, R. H., Rapid formation of plasma protein corona critically affects nanoparticle pathophysiology. Nat. Nanotechnol. 2013, 8 (10), 772-U1000.
6. Foroozandeh, P.; Aziz, A. A., Merging Worlds of Nanomaterials and Biological Environment: Factors Governing Protein Corona Formation on Nanoparticles and Its Biological Consequences. Nanoscale Res Lett 2015, 10.
7. Frank, M. M.; Fries, L. F., The role of complement in inflammation and phagocytosis. Immunol. Today 1991, 12 (9), 322-6.
8. Lesniak, A.; Salvati, A.; Santos-Martinez, M. J.; Radomski, M. W.; Dawson, K. A.; Aberg, C., Nanoparticle Adhesion to the Cell Membrane and Its Effect on Nanoparticle Uptake Efficiency. J. Am. Chem. Soc. 2013, 135 (4), 1438-1444.
9. (a) Li, S. D.; Huang, L., Stealth nanoparticles: High density but sheddable PEG is a key for tumor targeting. J. Controlled Release 2010, 145 (3), 178-181; (b) Niidome, T.; Yamagata, M.; Okamoto, Y.; Akiyama, Y.; Takahashi, H.; Kawano, T.; Katayama, Y.; Niidome, Y., PEG-modified gold nanorods with a stealth character for in vivo applications. J. Controlled Release 2006, 114 (3), 343-347; (c) Perry, J. L.; Reuter, K. G.; Kai, M. P.; Herlihy, K. P.; Jones, S. W.; Luft, J. C.; Napier, M.; Bear, J. E.; DeSimone, J. M., PEGylated PRINT Nanoparticles: The Impact of PEG Density on Protein Binding, Macrophage Association, Biodistribution, and Pharmacokinetics. Nano Lett. 2012, 12 (10), 5304-5310.
10. Bazile, D.; Prud'homme, C.; Bassoullet, M. T.; Marlard, M.; Spenlehauer, G.; Veillard, M., Stealth Me.PEG-PLA nanoparticles avoid uptake by the mononuclear phagocytes system. J. Pharm. Sci. 1995, 84 (4), 493-8.
11. Gref, R.; Minamitake, Y.; Peracchia, M. T.; Trubetskoy, V.; Torchilin, V.; Langer, R., Biodegradable long-circulating polymeric nanospheres. Science 1994, 263 (5153), 1600-3.
12. (a) Bradshaw, M.; Clemons, T. D.; Ho, D.; Gutierrez, L.; Lazaro, F. J.; House, M. J.; Pierre, T. G. S.; Fear, M. W.; Wood, F. M.; Iyer, S., Manipulating directional cell motility using intracellular superparamagnetic nanoparticles. Nanoscale 2015, 7 (11), 4884-4889; (b) Tangudu, N. K.; Verma, V. K.; Clemons, T. D.; Beevi, S. S.; Hay, T.; Mahidhara, G.; Raja, M.; Nair, R. A.; Alexander, L. E.; Patel, A. B.; Jose, J.; Smith, N. M.; Zdyrko, B.; Bourdoncle, A.; Luzinov, I.; Iyer, K. S.; Clarke, A. R.; Dinesh Kumar, L., RNA Interference Using c-Myc-Conjugated Nanoparticles Suppresses Breast and Colorectal Cancer Models. Mol. Cancer Ther. 2015, 14 (5), 1259-69.

13. Clemons, T. D.; Viola, H. M.; House, M. J.; Iyer, K. S.; Hool, L. C., Examining Efficacy of "TAT-less" Delivery of a Peptide against the L-Type Calcium Channel in Cardiac Ischemia-Reperfusion Injury. ACS Nano 2013, 7 (3), 2212-2220.

14. Iyer, K. S.; Zdyrko, B.; Malz, H.; Pionteck, J.; Luzinov, I., Polystyrene layers grafted to macromolecular anchoring layer. Macromolecules 2003, 36 (17), 6519-6526.

15. (a) Akinc, A.; Thomas, M.; Klibanov, A. M.; Langer, R., Exploring polyethylenimine-mediated DNA transfection and the proton sponge hypothesis. J. Gene Med. 2005, 7 (5), 657-663; (b) Al-Dosari, M. S.; Gao, X., Nonviral Gene Delivery: Principle, Limitations, and Recent Progress. AAPS J. 2009, 11 (4), 671-681.

16. (a) Hunter, A. C., Molecular hurdles in polyfectin design and mechanistic background to polycation induced cytotoxicity. Adv. Drug Delivery Rev. 2006, 58 (14), 1523-1531; (b) Moghimi, S. M.; Symonds, P.; Murray, J. C.; Hunter, A. C.; Debska, G.; Szewczyk, A., A two-stage poly(ethylenimine)-mediated cytotoxicity: Implications for gene transfer/therapy. Mol. Ther. 2005, 11 (6), 990-995.

17. Evans, C. W.; Fitzgerald, M.; Clemons, T. D.; House, M. J.; Padman, B. S.; Shaw, J. A.; Saunders, M.; Harvey, A. R.; Zdyrko, B.; Luzinov, I.; Silva, G. A.; Dunlop, S. A.; Iyer, K. S., Multimodal analysis of PEI-mediated endocytosis of nanoparticles in neural cells. ACS Nano 2011, 5 (11), 8640-8648.

18. (a) Hughes, M. M.; Field, R. H.; Perry, V. H.; Murray, C. L.; Cunningham, C., Microglia in the Degenerating Brain are Capable of Phagocytosis of Beads and of Apoptotic Cells, But Do Not Efficiently Remove PrPSc, Even Upon LPS Stimulation. Glia 2010, 58 (16), 2017-2030; (b) Stansley, B.; Post, J.; Hensley, K., A comparative review of cell culture systems for the study of microglial biology in Alzheimer's disease. J. Neuroinflammation 2012, 9; (c) Taylor, D. L.; Diemel, L. T.; Pocock, J. M., Activation of microglial group III metabotropic glutamate receptors protects neurons against microglial neurotoxicity. J. Neurosci. 2003, 23 (6), 2150-2160.

19. Boulos, S. P.; Davis, T. A.; Yang, J. A.; Lohse, S. E.; Alkilany, A. M.; Holland, L. A.; Murphy, C. J., Nanoparticle-Protein Interactions: A Thermodynamic and Kinetic Study of the Adsorption of Bovine Serum Albumin to Gold Nanoparticle Surfaces. Langmuir 2013, 29 (48), 14984-14996.

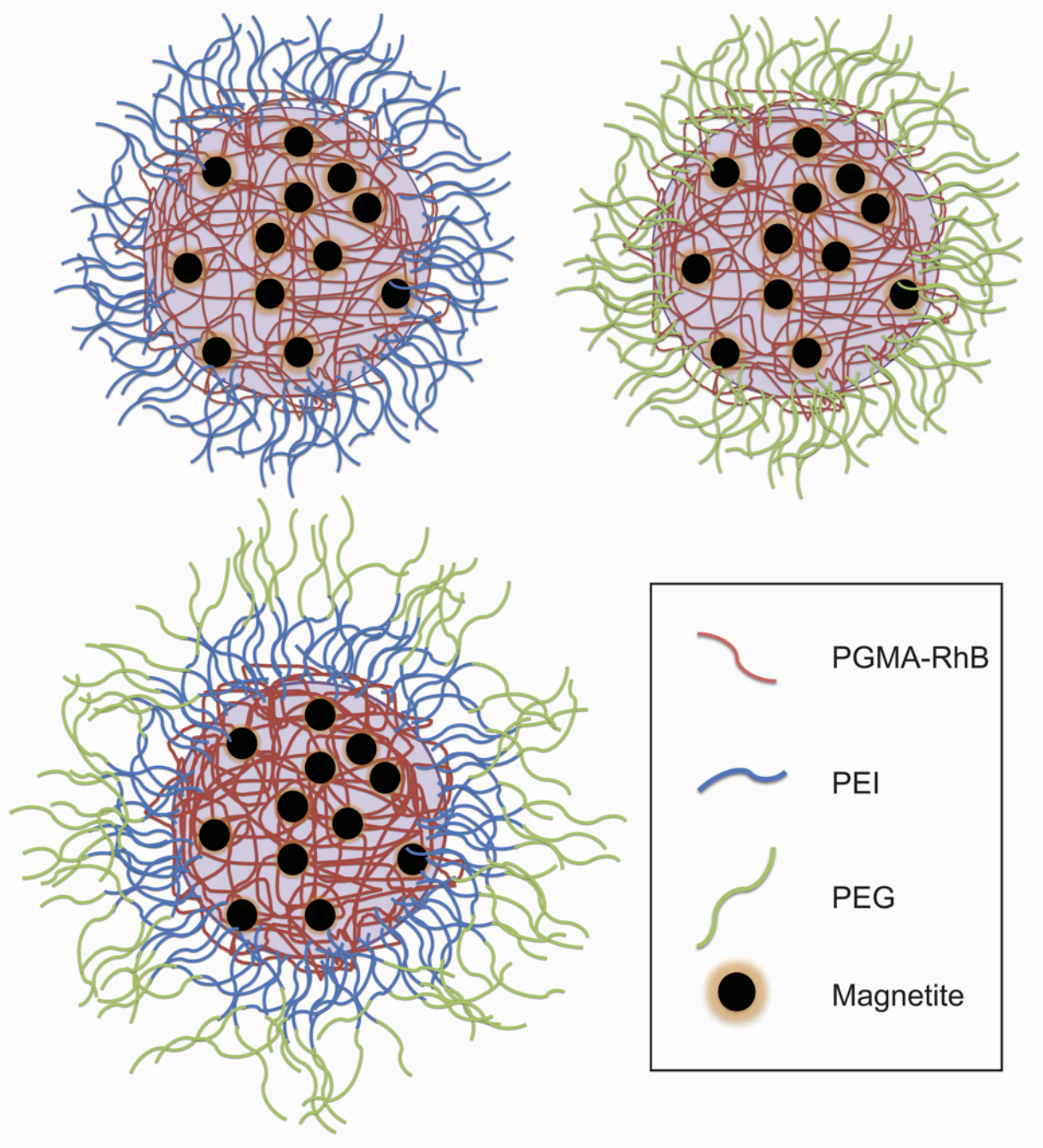

Table of Contents artwork

Manipulating cellular interactions of poly(glycidyl methacrylate) nanoparticles using mixed polymer brushes

Tristan D. Clemons,[a]* Michael Challenor,[a,b] Melinda Fitzgerald,[b] Sarah A. Dunlop,[b] Nicole M. Smith,[b] and K. Swaminathan Iyer[a]*

[a] School of Chemistry and Biochemistry, University of Western Australia, 35 Stirling Hwy, Crawley, WA 6009, Australia. Email: TDC: tristan.clemons@uwa.edu.au or KSI: swaminatha.iyer@uwa.edu.au
[b] School of Animal Biology, University of Western Australia, 35 Stirling Hwy, Crawley, WA 6009, Australia.

Supporting Information

Detailed Nanoparticle synthesis protocols

Materials: Solvents used in these experiments were of analytical grade. All chemicals were purchased from Sigma-Aldrich unless otherwise stated: benzyl ether (99%), Hexamethylene diisocyanate (HMDI), iron(III) acetylacetonate (97%), oleic acid (BDH, 92%), oleyl amine (70%), monomethyl ether poly(ethylene glycol) (mPEG, 5kDa), Pluronic F108, carboxylic end functionalized linear poly(ethylene glycol) (COOH-PEG) and poly(glycidyl methacrylate) (PGMA) were provided by Bogdan Zdyrko and Igor Luzinov, Clemson University, polyethylenimine (50% solution, M_n 1200, M_w 1300), rhodamine B (Kodak, 95%), and 1,2-tetradecanediol (90%) were used as received.

Preparation of magnetite nanoparticles: Magnetite (Fe_3O_4) was synthesised by the organic decomposition of $Fe(acac)_3$ in the presence of oleic acid, oleyl amine, and 1,2-tetradecanediol, in benzyl ether at 300 °C, as previously described by Sun et. al. for producing 6 nm particles.[1]

PEG-PEI Copolymer synthesis: The PEG-PEI copolymer was synthesized by following the protocol outlined by Peterson et al.[2] This protocol made use of a monomethyl ether 5kDa linear PEG which was activated with Hexamethylene diisocyanate (HMDI) before being reacted with a 25kDa branched PEI to produce the PEG-PEI copolymer. Briefly, 15.23g of mPEG 5kDa was dissolved in 15 mL $CHCl_3$ and reacted with 60 mL of HMDI under reflux (24h). The polymer was precipitated in petrol (750 mL), washed and redissolved in $CHCL_3$. The product was precipitated a further 10 times before collection and drying under vacuum of the final white solid product. 0.73 g of the activated mPEG was dissolved in 50 mL of $CHCl_3$ and combined with PEI 25 kDa (2.19g, 150 mL $CHCl_3$), refluxed for

24h to produce a waxy solid product used for conjugation to the PGMA nanoparticles.

RhB-grafting to PGMA: A solution of RhB (20 mg) and PGMA (100 mg) in MEK (20 mL) was heated to reflux under N_2 for 5 h. The modified polymer was concentrated in MEK *via* rotovap before being precipitated by the addition of diethyl ether (20 mL).

PEG-grafting to PGMA (for the PEG-PGMA nanoparticles): Similar to the RhB grafting a 5 kDa carboxylic end functionalized poly(ethylene glycol) (PEG-COOH, 40 mg) was added to RhB modified PGMA (100 mg) in MEK (20 mL) and heated to reflux under N_2 for 18 h. The modified polymer was concentrated in MEK *via* rotovap before being precipitated by the addition of diethyl ether (20 mL). This process was repeated to purify the final product before nanoparticle synthesis.

Polymer nanoparticle synthesis: Nanoparticles were prepared using a non-spontaneous emulsification route. The organic phase was prepared by dispersing iron oxide nanoparticles (20 mg) and dissolving PGMA–RhB (or the PGMA-RhB-PEG for the PEG only nanoparticles) (75 mg) in a 1:3 mixture of chloroform and MEK (6 mL). The organic phase was added dropwise, with rapid stirring, to an aqueous solution of Pluronic F108 (1.25% w/v, 30 mL) and the emulsion was homogenised with a probe-type ultrasonicator at low power for 1 min. The organic solvents were allowed to evaporate overnight under a slow flow of N_2. Centrifugation at 3000*g* for 45 min removed large aggregates of iron oxide and excess polymer. The supernatant was removed to a 50 mL flask containing either PEI (50 wt % solution, 100 mg) or the mPEG-PEI copolymer (100 mg) and heated to 80 °C for 18 h. The magnetic polymeric nanospheres were collected on a magnetic separation column (LS, Miltenyi Biotec), washed with water (2 × 1.5 mL), and then flushed with water until the filtrate ran clear to ensure all excess RhB and unattached polymer are removed. The resulting concentrated particle suspension was aliquoted (ca. 10 × 500 μl) and stored at 4 °C for quantification by lyophilisation, analysis and subsequent use.

Figure S1

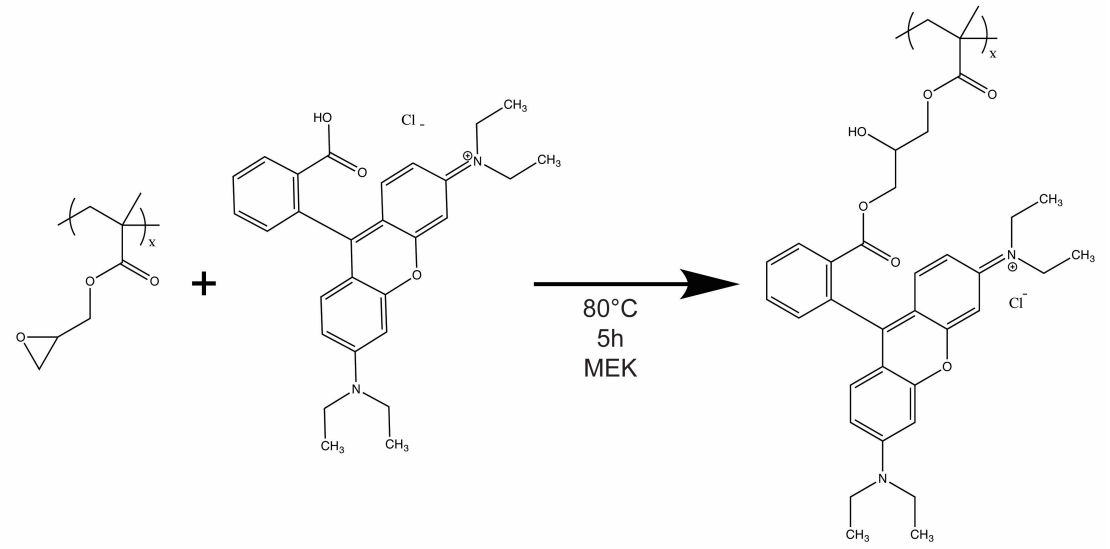

Figure S1 Reaction scheme for the synthesis of PGMA-RhB.

Figure S2

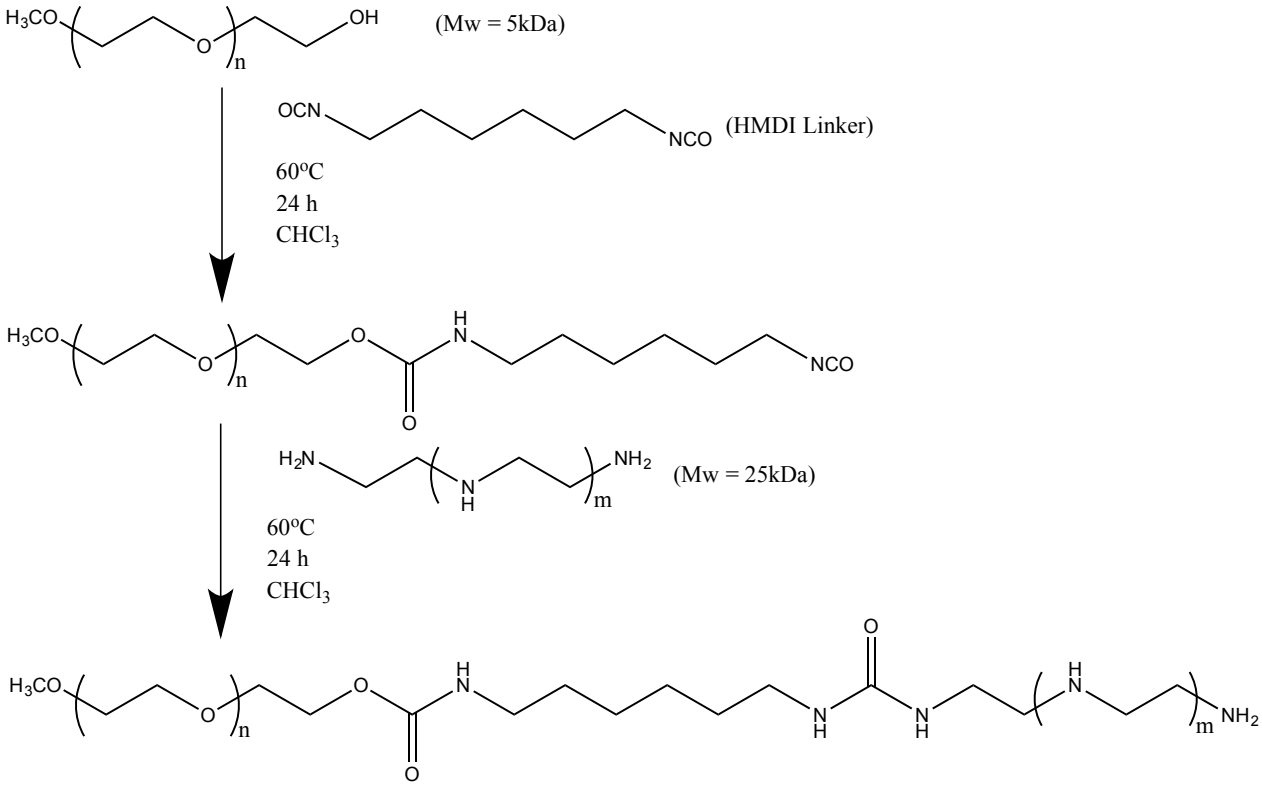

Figure S2 Reaction scheme for the synthesis of mPEG-PEI.[2]

Figure S3

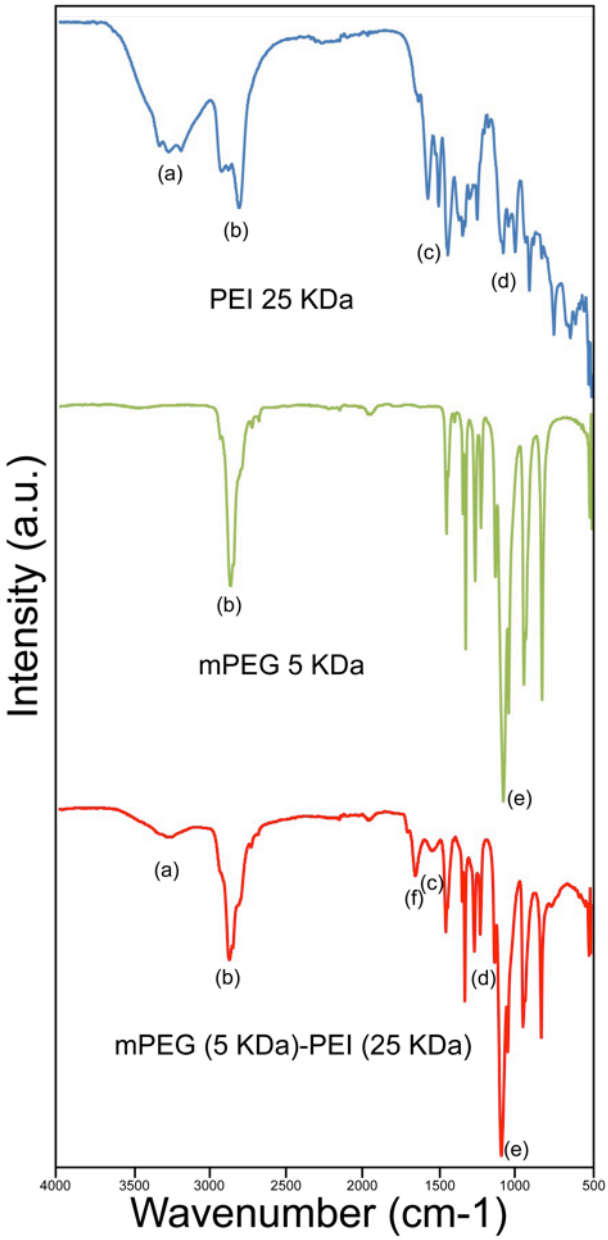

Figure S3 FTIR spectra of the 25kDa PEI (blue), 5kDa mPEG (green) and the mPEG-PEI copolymer (red) with characteristic bands for each spectra highlighted. (a) N-H stretch, (b) C-H stretch, (c) N-H bend, (d) C-N stretch, (e) C-O ether stretch and (f) C=O stretch.

Figure S4

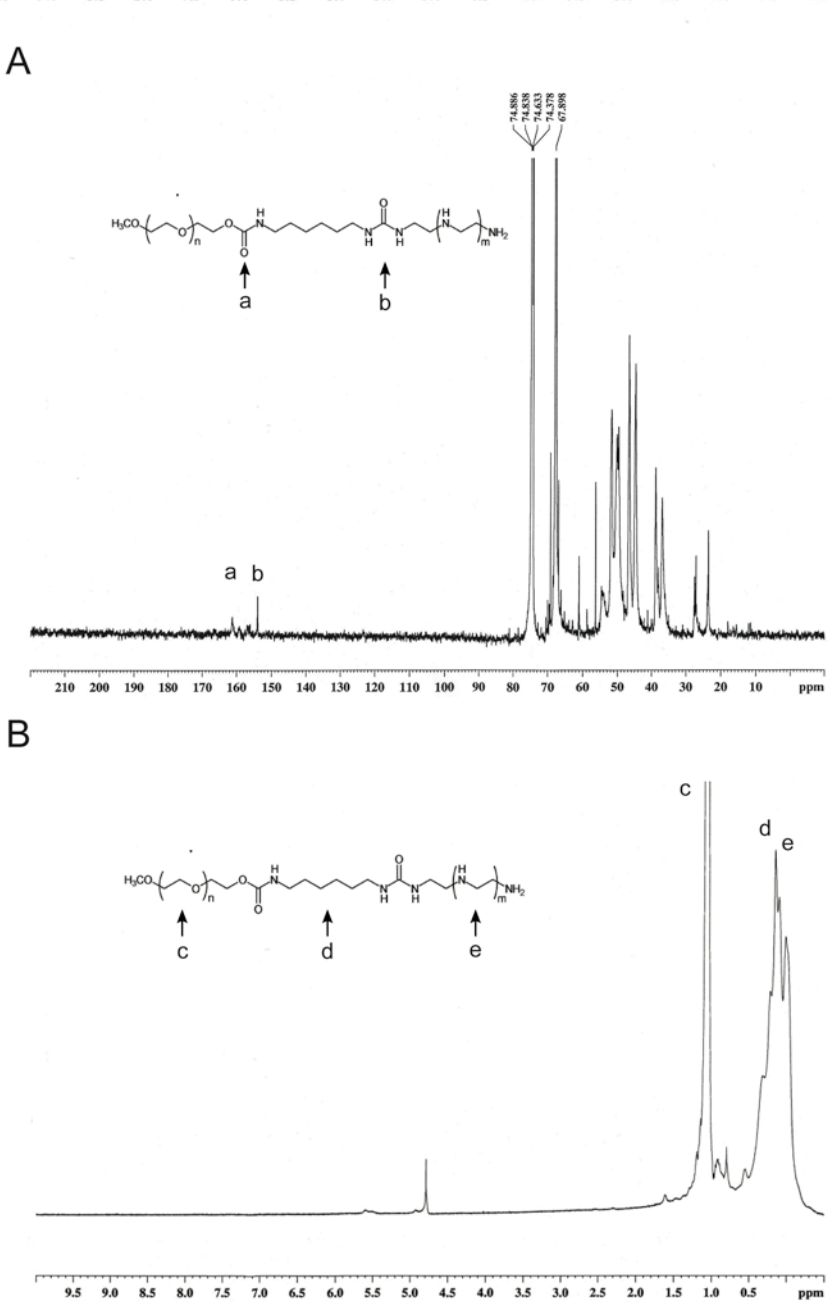

Figure S4 A) ^{13}C NMR in D2O of mPEG-PEI copolymer product showing evidence of urea and urethane bonds indicating attachment of the HMDI linker to both mPEG and PEI. B) ^{1}H NMR shows presence of proton signals arising from mPEG, HMDI linker and PEI.

Figure S5

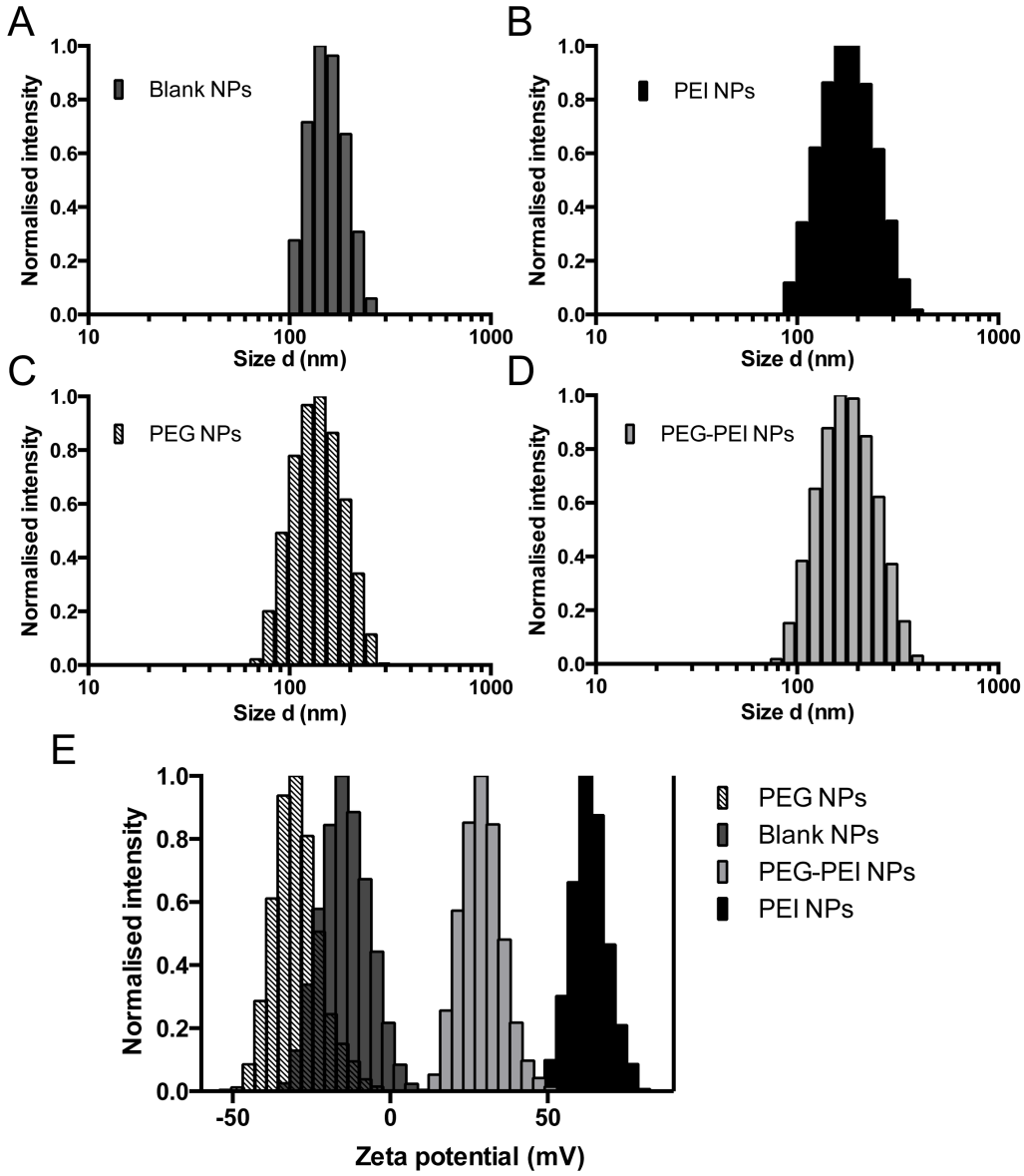

Figure S5 Dynamic light scattering assessment of nanoparticle size for A) unmodified 'blank' nanoparticles, B) PEI-decorated nanoparticles, C) PEG-decorated nanoparticles, D) mPEG-PEI-decorated nanoparticles and E) zeta potential analysis of each particle formulation in milli Q water.

Figure S6

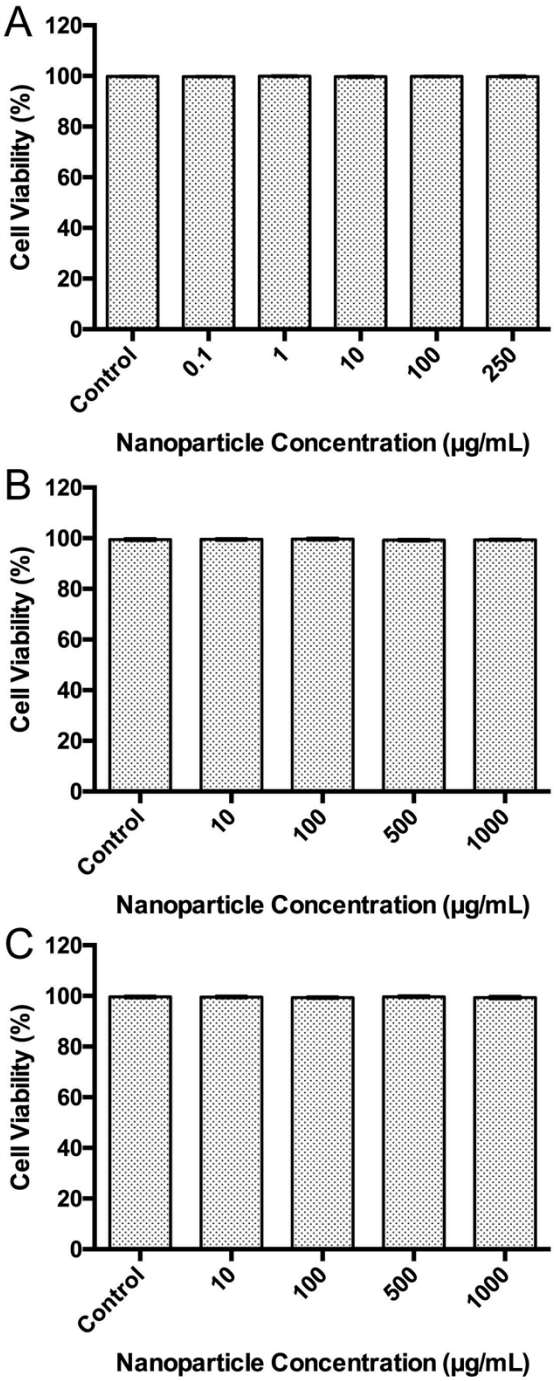

Figure S6 Toxicity assessment of nanoparticles after 24h incubation with PC12 cells at a range of concentrations for the A) PEI, B) PEG and C) mPEG-PEI decorated PGMA nanoparticles. n=3 wells as a minimum, and 4 fields of view per well for each concentration (between 1000 – 3000 cells counted per treatment). Data displayed as mean ± standard deviation. No significant differences were observed between all concentrations for each nanoparticle preparation, assessed with one-way ANOVA and Bonferroni-Dunn post hoc tests requiring significance $P \leq 0.05$.

Figure S7

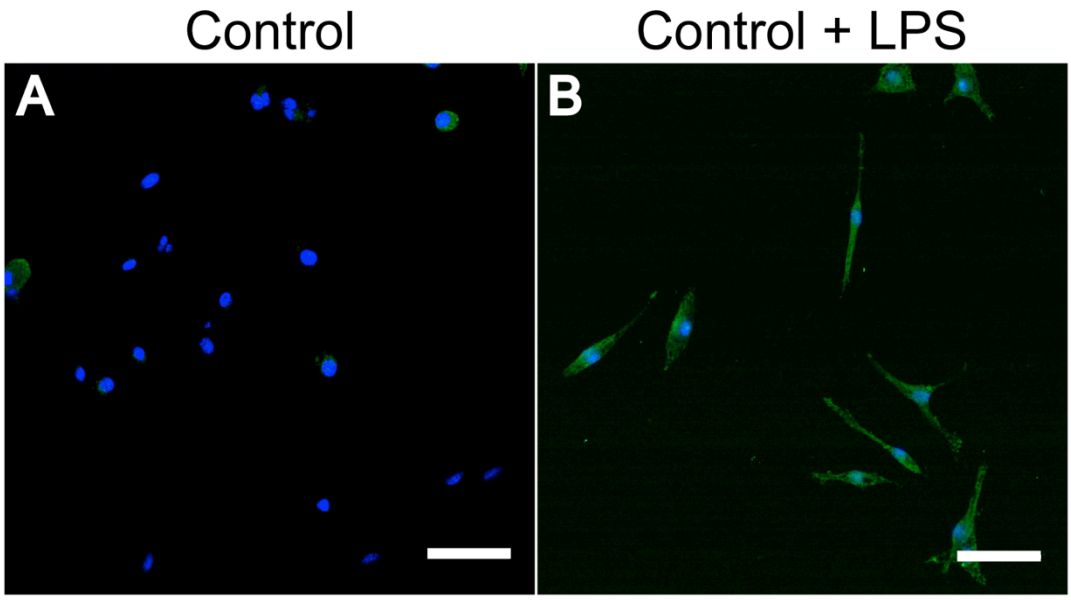

Figure S7 Control microglia (EOC2 CRL-2467) cells with and without activation achieved with 100 ng/ml lipolysaccharide (LPS), Hoescht (blue), ED1 (green), both scale bars are 50 μm.

Figure S8

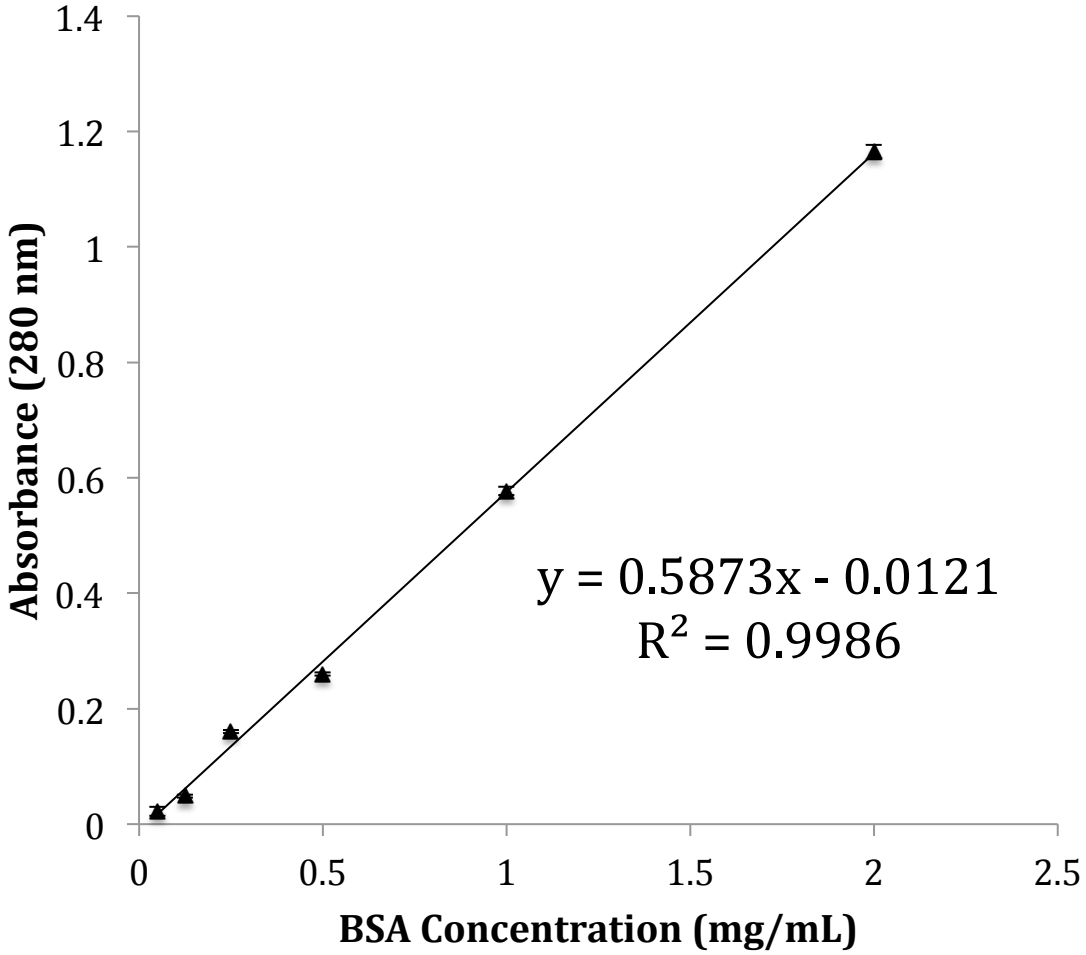

Figure S8 BSA standard absorbance values measured in duplicate on the NanoDrop UV-Vis instrument. This standard curve was used for the calculation of BSA bound to nanoparticles.

Table S1. Dynamic light scattering (DLS) characterisation of nanoparticle size and zeta potential.

Sample	Solvent	Particle size (nm, PDI)	Zeta Potential (mV)
Blank particles	water	158, 0.124	-13.9 ± 7.7
PEI particles	water	172, 0.086	52.9 ± 23.2
PEG particles	water	132, 0.074	-29.9 ± 19.3
mPEG-PEI particles	water	164, 0.111	29.0 ± 6.6
PEI particles	10% human serum	212, 0.219	-14.3 ± 3.6
PEG particles	10% human serum	232, 0.250	-10.3 ± 5.0
mPEG-PEI particles	10% human serum	248, 0.245	-7.75 ± 5.6
PEI particles	0.5 mg/ml BSA	207, 0.164	-30.8 ± 20.2
PEG particles	0.5 mg/ml BSA	241, 0.216	-22.6 ± 15.0
mPEG-PEI particles	0.5 mg/ml BSA	248, 0.256	-42.4 ± 20.3

Supporting Information References

1. S. Sun, H. Zeng, D. Robinson, S. Raoux, P. Rice, S. Wang and G. Li, *J. Am. Chem. Soc.*, 2004, **126**, 273-279.
2. H. Peterson, P. Fechner, D. Fischer and T. Kissel, *Macromolecules*, 2002, **35**, 6867-6874.